

**Cyclodextrin/poly(anhydride) nanoparticles as drug carriers for the oral delivery of atovaquone**

Javier Calvo<sup>a</sup>, José L. Lavandera<sup>a</sup>, Maite Agüeros<sup>b</sup>, Juan M. Irache<sup>b</sup>

<sup>a</sup> GlaxoSmithKline R&D, Diseases of the Developing World (DDW), Tres Cantos Medicines Development Campus, 28760 Tres Cantos, Spain

<sup>b</sup> Department of Pharmaceutics and Pharmaceutical Technology, School of Pharmacy, University of Navarra. 31080 Pamplona, Spain

**Corresponding author:**

Dr. Juan M. Irache  
Dep. Pharmaceutics and Pharmaceutical Technology  
University of Navarra  
31080 – Pamplona  
Spain  
Tel: +34948425600  
Fax: +34948425649  
e-mail: jmirache@unav.es

## **Abstract**

The aim was to study the ability of bioadhesive cyclodextrin-poly(anhydride) nanoparticles as carriers for the oral delivery of atovaquone (ATO). In order to increase the loading capacity of ATO by poly(anhydride) nanoparticles, the following oligosaccharides were assayed: 2-hydroxypropyl- $\beta$ -cyclodextrin (HPCD), 2,6-di-O-methyl- $\beta$ -cyclodextrin (DMCD), randomly methylated- $\beta$ -cyclodextrin (RMCD) and sulfobutyl ether- $\beta$ -cyclodextrin (SBECD). Nanoparticles were obtained by desolvation after the incubation between the poly(anhydride) with the ATO-cyclodextrin complexes. For the pharmacokinetic studies, ATO formulations were administered orally in rats. Overall, ATO displayed a higher affinity for methylated cyclodextrins than for the other derivatives. However, for in vivo studies, both ATO-DMCD-NP and ATO-HPCD-NP were chosen. These nanoparticle formulations showed more adequate physicochemical properties in terms of size (< 260 nm), drug loading (17.8 and 16.9  $\mu\text{g}/\text{mg}$ , respectively) and yield (>75%). In vivo, nanoparticle formulations induced higher and more prolonged plasmatic levels of atovaquone than control suspensions of the drug in methylcellulose. Relative bioavailability of ATO when loaded in nanoparticles ranged from 52% (for ATO-HPCD NP) to 71% (for ATO-DMCD NP), whereas for the suspension control formulation the bioavailability was only about 30%. The encapsulation of atovaquone in cyclodextrin-poly(anhydride) nanoparticles seems to be an interesting strategy to improve the oral bioavailability of this lipophilic drug.

## **Keywords**

Atovaquone, nanoparticles, cyclodextrin, bioadhesion, oral delivery.

## Introduction

Atovaquone is a 1,4-hydroxynaphthoquinone with broadspectrum antiprotozoan activity, including demonstrated efficacy against *Pneumocystis carinii* (Hughes et al. 1993), *Toxoplasma gondii* (Araujo et al. 1991; Kovacks 1992), *Plasmodium* species (Looareesuwan et al. 1996; Radloff et al. 1996), *Babesia* spp. (Matsuu et al. 2004) and *Leishmania* spp. (Murray and Hariprashad 1996; Cauchetier et al. 2002).

Atovaquone, as a structural analog of ubiquinone, induces a potent inhibitory effect in the respiratory chain of parasites (Gutteridge 1991). The site of action is believed to be the cytochrome *bc1* complex (complex III), in which the drug would affect some metabolic enzymes, such as dihydroorotate dehydrogenase (Ittarat et al. 1995), that are linked to the mitochondrial electron transport chain by ubiquinone. Interestingly, it was demonstrated that the inhibition of respiration of mitochondria from protozoan was about 1000-fold more sensitive than were mammalian and avian mitochondria (Kessl et al. 2003).

Atovaquone was proposed as an alternative agent for the treatment of both mild and moderate *Pneumocystis carinii* pneumonia (PCP) in acquired immune deficiency syndrome (AIDS) patients and was registered as Mepron® for this indication (Sherman 2009). This drug was also found effective against toxoplasmosis, another common opportunistic infection in patients with AIDS (Spencer and Goa 1995). In this case, atovaquone displays a potent in vitro activity against both the tachyzoite and cyst forms of *Toxoplasma gondii* (Romand et al. 1993; Ferguson et al. 1994).

Furthermore, atovaquone was also proposed for the treatment of malaria. In fact, it was found to be much more active than the standard anti-malarials in cultures of *Plasmodium falciparum* and against *P. berghei* and *P. yoelii* in mice (Hudson 1993). More interestingly, this antiprotozoan was found curative when administered orally in Aotus monkeys infected with *P. falciparum* (Hudson 1993). However, when it was used as monotherapy for *P. falciparum* infections there was a 30% treatment failure rate with atovaquone-resistant parasites emerging 28 days after treatment (Kessl et al. 2007). To counter this problem it has been combined with proglanil hydrochloride (Malarone®) and the combination has been found to be effective in areas where parasites are resistant to mefloquine, chloroquine, or sulphadoxinepyrimethamine (Kessl et al. 2007). Another important advantage of this antiprotozoan is related with its tolerability and the absence of severe side effects that would require withdrawal of the therapy. The most common reactions are rash, fever, vomiting, diarrhoea, abdominal pain and headache (Sherman 2009).

From a physico-chemical point of view, atovaquone is a highly lipophilic substance (Log P= 5) with a poor solubility (<0.2 µg/ml) in aqueous media such as gastrointestinal fluids (Dressman and Reppas 2000). Thus, when administered orally in a conventional form (i.e. tablet or suspension), this drug is irregularly absorbed and it shows a very poor bioavailability. However, absorption of ATO can be improved by the simultaneous intake of food (Hughes et al. 1991; Rolan et al. 1994). Thus, the oral bioavailability of atovaquone has been calculated to be about 23% in the fasted state and 47% in the fed state (GlaxoSmithKline 2010).

This influence of food in absorption and the high production costs of the drug hamper its use in developing countries. Nevertheless atovaquone is now the benchmark anti-malarial chemoprophylactic for the traveller market (Sherman 2009).

In order to improve the oral bioavailability of atovaquone some different attempts have been proposed, including its formulation in self-microemulsifying drug delivery systems (Sek et al. 2008), nanocapsules (Sordet et al. 1998; Cauchetier et al. 2003) and solid nanoparticles (Dearn 2000). Another alternative to improve the oral bioavailability of drugs can be the use of bioadhesive nanoparticles, such as poly(methylvinylether-co-maleic anhydride) or PVM/MA nanoparticles (Arbos et al. 2002). The development of adhesive interactions can be of interest to increase the residence time of the drug delivery system in close contact with the absorptive membrane. This fact would facilitate the establishment of a concentration gradient between the pharmaceutical dosage form and the absorptive membrane increasing the possibilities for drug absorption. However, in our case, the capability of PVM/MA nanoparticles to load highly lipophilic drugs (i.e. atovaquone) is limited. In order to minimise this drawback, one possible solution may be the incorporation of cyclodextrins as promoters of drug loading for the preparation of nanoparticles. The resulting cyclodextrin-PVM/MA nanoparticles have been proven effective to both develop intense bioadhesive interactions between the gut (Agüeros et al., 2009a) and to increase the drug loading of lipophilic drugs such as paclitaxel (Agüeros et al. 2009b).

The aim of this work was to study the ability of cyclodextrin-PVM/MA

nanoparticles as carriers for the oral delivery of atovaquone. For this purpose, the following oligosaccharides were assayed: 2-hydroxypropyl- $\beta$ -cyclodextrin, randomly methylated  $\beta$ -cyclodextrin, 2,6-di-O-methyl- $\beta$ -cyclodextrin and sulfobutyl ether- $\beta$ -cyclodextrin. In addition, the ability of these nanoparticles to increase the oral bioavailability of atovaquone was evaluated in laboratory animals.

## **2. Material and methods**

### **2.1. Chemicals**

Poly(methylvinyl ether-co-maleic anhydride) or PVM/MA [Gantrez<sup>®</sup> AN119; MW 200 000] was kindly gifted by ISP (Barcelona, Spain). Atovaquone (ATO) was provided by ChemPacific Corp (Baltimore, USA). 2-hydroxypropyl- $\beta$ -cyclodextrin (HPCD) and randomly methylated  $\beta$ -cyclodextrin (RMCD) were purchased from Sigma-Aldrich (Steinheim, Germany), 2,6-di-O-methyl- $\beta$ -cyclodextrin (DMCD) from ABCR (Karlsruhe, Germany) and sulfobutyl ether- $\beta$ -cyclodextrin (SBECD) [Captisol<sup>®</sup>] from Cydex Inc. (Lenexa, USA). All the solvents and reagents used for preparation, characterisation and analysis of nanoparticles were of analytical grade and were obtained from Merck (Darmstadt, Germany) and Sigma-Aldrich (Steinheim, Germany). All the aqueous solutions were prepared using purified distilled water from Millipore Milli-Q system (Bedford MA, USA).

### **2.2. Solubility studies**

According to Higuchi and Connors method (Higuchi and Connors 1965), solubility studies were carried out in aqueous media at 25°C. The cyclodextrins used were HPCD, RMCD, DMCD and SBECD. An excess of ATO was added to PBS (0.14 M NaCl, 0.0027 M KCl, 0,01 M phosphate buffer pH 7.4 at 25°C) containing increasing amounts of cyclodextrins. These suspensions were shaken under magnetic stirring at 25°C until solubility equilibrium was reached (7 days). Then, the samples were filtered (0.45 µm) and the concentration of ATO was determined by UPLC-UV (see section 2.6.2). The presence of trace amounts or cyclodextrins did not interfere with the assay. The assays were performed in triplicate.

The apparent stability constant ( $K_c$ ) according to the hypothesis of 1:1 stoichiometric ratio of complexes was calculated from the phase solubility diagrams using the following equation (Higuchi and Connors 1965):

$$K_c = \frac{Slope}{S_0 \times (1 - Slope)} \quad [Eq. 1]$$

The slope is obtained from the initial straight-line portion of the plot of atovaquone concentration against cyclodextrin concentration, and  $S_0$  is the equilibrium solubility of atovaquone in the aqueous media.

In addition, the complexation efficiency (CE) was calculated. This parameter is determined either from the slope of the phase-solubility profile or the complex to free cyclodextrin concentration ratio, which is referred to as the complexation efficiency (Loftsson et al. 2005):

$$CE = S_0 \times K_c = \frac{[D/CD]}{[CD]} = \frac{Slope}{1 - Slope} \quad [Eq. 2]$$

where  $[D/CD]$  is the concentration of dissolved complex,  $[CD]$  is the concentration of dissolved free cyclodextrin and Slope is the slope of the phase-solubility profile.

### **2.3. Preparation of ATO loaded-nanoparticles**

Nanoparticles, containing the atovaquone-cyclodextrin complexes (ATO-CD), were prepared by a modification of a solvent displacement method previously described (Agüeros et al. 2009a). For this purpose, 20 mg of cyclodextrin and 2.5 mg of ATO were dissolved in 10 ml of ethanol and maintained under agitation for 30 minutes at room temperature. Meanwhile, 100 mg of PVM/MA or poly(anhydride) were dissolved in 5 ml of acetone. Then the nanoparticles were formed after addition of the ethanol solution containing cyclodextrin and ATO to the polymer phase in acetone. After that, 10 ml of desionized water was added and the organic solvents were removed under reduce pressure (Büchi R-14, Switzerland). The resulting carriers were purified by centrifugation at 27,000 x g for 20 min. The supernatants were removed and the pellets resuspended in water. The purification procedure was repeated twice and finally, the formulations were frozen and then freeze-dried (Genesis 12EL, Virtis, USA) using sucrose (5% w/w) as cryoprotector.

Empty poly(anhydride) nanoparticles, used as control, were prepared in the same way in the absence of ATO.

### **2.4. Preparation of ATO suspension**

A large amount of 50 mg of ATO was firstly pulverised in a planetary ball-mill

(MM200, Restch, Düsseldorf, Germany). Then, 5 mg of the resulting powder was weighed and homogeneously dispersed under magnetic agitation at room temperature in 20 ml of an aqueous solution of methyl cellulose (1% w/v). The size of the suspension was assessed by a Zetamaster Analyser system (Malvern, UK).

Before the administration to animals, the amount of drug dispersed in the suspension was assessed by Ultra Performance Liquid Chromatography (UPLC), (see section 2.6.2).

## **2.5. Preparation of ATO intravenous solution**

An amount of 3 mg of pulverised ATO was completely dissolved by agitation in 1 ml of DMSO. Meanwhile, a 5 ml of HPCD solution at a final concentration of 40% (w/v) was prepared. Then, 100 µl of ATO solution in DMSO were added to 5 ml of the cyclodextrin preparation. The resulting solution was kept under magnetic agitation for 10 minutes and visual inspected to confirm the absence of solid particles or agglomerates. Then, the necessary volume of saline (0.9% NaCl) was added under agitation to a final volume of 10 ml. Finally, this solution was filtered by 0.2 µm PTFE filters (Millipore, Milford, USA) and kept in sealed vials till use.

## **2.6. Characterisation of nanoparticles**

### **2.6.1. Particle size, zeta potential, morphology and yield**

The size and zeta potential of nanoparticles were measured by photon correlation spectroscopy and Laser Doppler Anemometry respectively, using a

Zetamaster Analyser system (Malvern Instruments, USA). Size measurements were performed at 25°C and at a 90° scattering angle, and each measurement was recorded for 90 s. The mean hydrodynamic diameter was generated by cumulative analysis. The zeta potential measurements were performed with an aqueous dip cell in the automatic mode.

The morphology and shape of the nanoparticles were examined by scanning electron microscopy (SEM) in a Hitachi S3000-N (Hitachi HTA, Inc., Pleasanton, CA, USA). For this purpose freeze-dried formulations were resuspended in ultrapure water and centrifuged at 27,000 x g for 20 minutes at 4 °C. Then, supernatants were removed and the obtained pellets were mounted on a glass plate, adhered with a double-sided adhesive tape onto metal stubs and coated with gold to a thickness of 8 nm (Polaron SC 502, Sputter Coater, UK). The micrographs were taken with the following conditions: 10 kV and 50000X from 9 mm distance.

The yield of the nanoparticles preparation process was determined by gravimetry from freeze-dried nanoparticles as described previously (Arbos et al. 2002).

### **2.6.2. Atovaquone content**

The amount of atovaquone loaded into nanoparticles was calculated by UPLC. Briefly, the apparatus was an UPLC Acquity with photodiode array detector (PDA) set at 254 nm. Data were collected and processed by chromatographic software MassLynx 4.1 (Waters). The chromatographic system was equipped with a reversed – phase 50 x 2.1 mm UPLC Acquity BEH C18 column (1.7 µm).

The gradient elution buffers were A (methanol and 0.1% formic acid) and B (water and 0.1% formic acid). The column was eluted with a linear gradient consisted of 90% A over 0.5 min, 90 to 10% over 0.5 to 4 min, 10% over 4 to 4.5 min, returned to 90 for 0.5 min and kept for a further 1 min before the next injection. Total run time was 5 min, volume injection was 5  $\mu$ l and the flow rate 500  $\mu$ l/min. ATO stock solution in methanol was refrigerated and calibration curves were designed over the range 0.1–100  $\mu$ g/ml ( $r^2 > 0.999$ ). The limit of quantification was calculated to be 0.5  $\mu$ g/ml with a relative standard deviation lower than 2.5%.

For analysis, 5 mg nanoparticles were digested with 1 ml acetonitrile. After filtering through 0.2  $\mu$ m PTFE filter, the samples were transferred to auto-sampler vials, capped and placed in the UPLC auto sampler. Then, 10  $\mu$ l aliquot was injected onto UPLC column. Each sample was assayed in triplicate and results were expressed as the amount of atovaquone (in  $\mu$ g) per mg nanoparticles. Similarly, the encapsulation efficiency (EE in percentage) was calculated as the ratio between the amount of drug entrapped in the nanoparticles and the initial amount of ATO used to prepare the nanoparticle batch.

## **2.7. Administration of nanoparticle formulations, oral suspensions and intravenous solution to rats**

Male Wistar rats (average weight 225 g) (Harlan, Spain) were housed under normal conditions with free access to food and water. The animals were placed in metabolic cages and fasted overnight to prevent coprophagia but allowing

free access to water. The experiment was performed according to the policies and guidelines of the responsible Committee of the University of Navarra in line with the European legislation on animal experiments (86/609/EU).

For the pharmacokinetics study, the rats were divided at random in five groups (n=5). First group received ATO (0.15 mg/kg, 5 ml/kg) by intravenous injection through tail vein. The other groups of animals received ATO (2.5 mg/Kg, 10 ml/kg) in different formulations by oral administration: (a) ATO suspension in 1% methyl cellulose; (b) ATO suspension in 1% methyl cellulose containing empty nanoparticles; (c) ATO-HPCD complexes loaded in nanoparticles; (d) ATO-DMCD complexes loaded in nanoparticles.

Blood samples (~0.1 ml) were collected in tubes containing EDTA (Vacuette® EDTA K2) at 0.08, 0.25, 0.5, 1, 2, 5, 10, 24 and 48 h following iv administration and 0.25, 0.5, 1, 2, 5, 10, 24, 48 and 96 h following oral administration. The volemia was recovered via intraperitoneal with an equal volume of normal saline solution preheated at body temperature. Blood samples were immediately frozen at -80°C for posterior analysis.

## **2.8. Analysis of ATO in blood samples**

### **2.8.1 Preparation of standard solutions**

A stock solution of ATO was firstly prepared by dissolution of 5 mg ATO in 50 ml DMSO. Further standard solutions were obtained by serial dilutions with DMSO. The calibration curve samples were prepared by spiking 28.5 µl of rat blood with 1.5 µl of the appropriate standard to obtain ATO final concentrations of 12.5, 25, 50, 125, 250, 500, 1250 and 2500 ng/ml. All the standard solutions

were above the lower limit of quantification and within a linear range of quantification. Peak area ratios of the ATO and internal standard were calculated and the calibration curves adjusted by fitting these ratios to the concentrations by a linear regression method.

### **2.8.2 Preparation of samples**

Blood samples and calibration standards were treated as follows: 30 µl of 0,1% saponin solutions were added to blood and shaken by vortex for 1 min. Protein precipitation was carried out after addition of 240 µl of an acetonitrile:methanol (1:2) mixture containing internal standard at 50 ng/ml. Then, samples were shaken by vortex for 1 minute and centrifuged at 15 000 rpm for 30 min. The supernatants were filtered through 0.2 µm filters to avoid the presence of solid particles and placed on 300 µl vials to be analysed by LC-MS/MS.

### **2.8.3. LC-MS/MS Conditions**

UPLC equipment was coupled to API2000 QTrap MS/MS system (Applied Biosystems/MDS SCIEX) equipped with an electrospray ionization (ESI) source operating with ion spray at -4500 V and heater temperature at 500°C. Nitrogen and zero grade air were employed. Gas settings were as follows: curtain gas 20 arbitrary units, collision gas 8 arbitrary units, nebulizer gas 40 arbitrary units, and heater gas 60 arbitrary units. Dwell time per transition was set at 100 ms. Nitrogen was set as curtain gas and collision gas in the Q2 collision cell. Unit mass resolution was set in both mass-resolving quadrupole Q1 and Q3. Data were processed by Analyst 1.4.1 Software package (MDS SCIEX, Canada).

Quantification by multiple reactions monitoring mode (MRM) analysis was performed in the negative ion mode. The declustering potential (DP) and the collision energy was set at -96 V. The MRM acquisition was performed at unit resolution using the transitions  $m/z$  364.9  $\rightarrow$  337.0.

## 2.9. Pharmacokinetic analysis

The pharmacokinetic analysis of blood concentration vs time data, obtained after administration of the different ATO formulations, was analysed using a noncompartmental model with the WinNonlin 5.2 software (Pharsight Corporation, Mountain View, US).

With this purpose, the following pharmacokinetic parameters were estimated from data obtained with animals of Group I: Total area under the curve from time 0 to  $\infty$  after intravenous administration ( $AUC_{iv}$ ), clearance (CL), volume of distribution in steady state ( $V_{ss}$ ), mean residence time (MRT) and half-life of the terminal phase ( $t_{1/2}$ ).

On the other hand, for oral administered formulations, other PK parameters were also calculated such as the peak of maximum concentration ( $C_{max}$ ) and the time to peak concentration ( $T_{max}$ ). Furthermore, the relative bioavailability (F %) of atovaquone was estimated using the ratio of dose-normalised AUC values following oral and iv administrations [Eq. 3]

$$F(\%) = \frac{D_{iv} \times AUC_{oral}}{D_{oral} \times AUC_{iv}} \quad [\text{Eq. 3}]$$

where  $D_{iv}$  and  $D_{oral}$  are the doses received by intravenous and by oral route respectively, and  $AUC_{oral}$  and  $AUC_{iv}$  are the area under the curve, after the oral and intravenous administration.

## 2.10. Statistical analysis

Data are expressed as the mean  $\pm$  S.D. of at least three experiments. The physico-chemical characteristics were compared using Student's t-test. For the pharmacokinetic studies, the Mann-Whitney U-test was used to investigate statistical differences. In all cases,  $p < 0.05$  was considered to be statistically significant. All data processing was performed using GraphPad Prism 4.0 statistical software program (GraphPad Software, La Jolla, USA).

## 3. Results

### 3.1. Solubility studies

Figure 1 shows the phase-solubility diagrams of ATO for the different cyclodextrins tested. For all the oligosaccharides, the solubility of the drug in the aqueous medium increased linearly as a function of the cyclodextrin concentration. The plots obtained for RMCD, HPCD and SBECD were typical of those ascribed to  $A_L$  type diagrams (Higuchi and Connors 1965). In fact, the linear host-guest correlations ( $r > 0.99$ ) suggested the formation of a 1:1 (ATO–cyclodextrin) complex with respect to cyclodextrin concentrations.

For the DMCD, the plot appeared to fit better to a  $B_S$  type diagram. Hence, in order to compare its capacity to enhance the atovaquone solubility with the other cyclodextrins, the slope and the complexation efficiency were calculated using only the initial ascending portion of the plot, where the concentration of cyclodextrin increased linearly with the amount of solubilised drug.

Table 1 summarises the apparent stability constant,  $K_c$ , obtained from the slope of the linear phase-solubility diagrams.  $K_c$  was found to be dependent on the nature of the cyclodextrin used. Thus, the higher  $K_c$  was observed for DMCD, which was found to be about 2-times higher than for HPCD or around 6-fold higher than for SBECD. The complexation efficiency constants were calculated to be about 0.002, 0.004, 0.006 and 0.010 for SBECD, HPCD, RMCD and DMCD respectively.

### **3.2. Physicochemical characterization of nanoparticles**

Table 2 summarises the main physico-chemical properties of the different atovaquone formulations evaluated in this study. For the atovaquone control suspension (see section 2.4), the mean size of particles dispersed was found to be about 640 nm. In any case, it was calculated that 92% of the drug particles were less than 857 nm and 38% were less than 615 nm. Comparing to empty nanoparticles (NP), the encapsulation of ATO slightly increased the size of the resulting nanoparticles (about 260 nm vs 240 nm, respectively), except when HPCD was used (about 200 nm). Interestingly, the polydispersity index (PDI) was found to be always lower than 0.2, which is considered as an evidence of a homogeneous nanoparticle formulation. The zeta potential of the ATO-loaded nanoparticles was found to be slightly less negative than for empty nanoparticles (about -46 mV vs -51 mV).

Figure 2 shows microphotographs of nanoparticles obtained by SEM. In all cases, the apparent size of nanoparticles was found to be similar to values

obtained by photon correlation spectroscopy. In addition, nanoparticles containing ATO displayed a spherical shape and a smooth surface (Figure 2).

Concerning the drug loading, the amount of ATO encapsulated in nanoparticles was found to be dependent on the type of cyclodextrin used. Thus, DMCD and HPCD displayed a higher ability to load atovaquone than when RMCD was used (around 17  $\mu\text{g}/\text{mg}$  vs 12.7  $\mu\text{g}/\text{mg}$ , respectively). In the absence of cyclodextrins, the amount of ATO loaded in PVM/MA nanoparticles was extremely low (below the limit of quantification by UPLC: 0.1  $\mu\text{g}$  ATO / mg NP).

### 3.3. Pharmacokinetic analysis

The plasma concentration profiles of atovaquone after a single intravenous administration at 150  $\mu\text{g}/\text{kg}$  formulated in DMSO/HPCD/saline are shown in Figure 3. The data were adjusted by non-compartmental model. The peak plasma concentration ( $C_{\text{max}}$ ) of atovaquone was  $525 \pm 115 \mu\text{gml}^{-1}$ . The mean values obtained for  $\text{AUC}_{0-\infty}$  and  $V_{\text{ss}}$  were  $11.1 \pm 4.5 \mu\text{gml}^{-1}\text{min}^{-1}$  and  $0.81 \pm 0.1 \text{ l kg}^{-1}$  respectively. Other pharmacokinetic parameters as clearance and half-life ( $C_{\text{L}} = 20.4 \pm 7.8 \text{ ml h}^{-1} \text{ kg}^{-1}$  and  $t_{1/2} = 30.6 \pm 13.6 \text{ h}$ ) showed a slow removal of the drug.

Figure 4 shows the plasma concentration profiles of atovaquone after a single oral administration of 2.5 mg/kg to laboratory animals when formulated either in nanoparticles or dispersed in a methylcellulose aqueous solution. Table 3 summarises the main pharmacokinetic parameters derived from these curves. The peak blood concentration ( $C_{\text{max}}$ ) of atovaquone when loaded in nanoparticles with DMCD was found to be significantly higher than when

dispersed in the aqueous solution of methylcellulose ( $p < 0.05$ ), although all the formulations appeared to show a similar  $T_{max}$ . Interestingly, the AUC of atovaquone in nanoparticles was about 2.2-fold higher than that in the suspension of methylcellulose. Similarly, the MRT of ATO when incorporated in nanoparticles was about 5 h longer than when dispersed in the conventional formulation.

Comparing the two nanoparticle formulations, it appears clear that the presence of DMCD provided a slightly higher ability than HPCD to promote the absorption of this drug. The calculated relative bioavailability of atovaquone delivered in nanoparticles was calculated to be about 71% for ATO-DMCD NP and 52% for ATO-HPCD NP. In both cases, these values were higher than the bioavailability observed for atovaquone when dispersed in the methylcellulose composition (about 31%). Finally, it is interesting to note that the incorporation of empty nanoparticles to the aqueous dispersion of atovaquone decreased the bioavailability of the drug.

#### **4. Discussion**

Atovaquone shows a high activity against several intra- and extracellular protozoa (Araujo et al. 1991; Hughes et al. 1993; Matsuu et al. 2004; Murray and Hariprashad 1996; Cauchetier et al. 2002) and, associated with proguanil, is currently used in malaria prophylaxis and treatment (Pelter and Kain 2005; Polhemus et al. 2008). From a biopharmaceutical point of view, atovaquone can be classified as a BCS class II, characterised by a high permeability and a low aqueous solubility (Dressman and Reppas 2000). In fact, this drug is a highly

lipophilic compound that, when administered by the oral route, shows a very variable absorption and a poor bioavailability. The dose to solubility ratio (D:S) for atovaquone in simulated intestinal fluids has been calculated to be as high as 80 liters (Nicolaidis et al. 1999). In this context, the selection and design of the appropriate drug delivery system has a key influence in the overall efficacy of the drug. Thus, for atovaquone, the formulation related factors such as the particle radius size or the presence of solubilising agents may be critical to modulate its oral absorption.

Atovaquone was firstly commercialised as tablets (Mepron®), from which it was far from a complete oral bioavailability (Nicolaidis et al. 1999). It was shown that, in the fed state, the absolute bioavailability of Mepron® tablets in HIV seropositive volunteers was about 21% (Nicolaidis et al. 1999). In 1995, the tablet was replaced with the suspension because of the superior bioavailability of the latter (Cotton 1995). In different clinical studies, it was confirmed that the concentration in plasma reached with a dose in suspension was two to three times greater than that reached with the same dose in tablet formulation in the fasting or fed state (Hughes et al. 1993; Dixon et al. 1996). This fact was explained by the size of atovaquone particles in the suspension which were significantly smaller than those produced after tablet disintegration.

Another key parameter influencing atovaquone absorption is its administration with food. Thus, it was demonstrated that, for both the tablet and suspension formulations, the atovaquone concentration in plasma is greater when the drug is administered with food (Rolan et al. 1994; Dixon et al. 1996). Overall, it has been calculated that food increases the bioavailability of atovaquone 1.4-fold

over that achieved in a fasting state (Rolan et al. 1994); although, this amount can be higher depending on the fat content of the meal (Nicolaidis et al. 1999). Other possibilities to increase the atovaquone oral bioavailability have been proposed, including the development of nanosuspensions (Dearn 2000; Nicolaidis et al. 1999), self-microemulsifying drug delivery systems (Sek et al. 2008), liposomes (Cauchetier et al. 2000) or polymer nanocapsules (Dalençon et al. 1997; Sordet et al. 1998; Cauchetier et al. 2002). All of these strategies are based on an increment of the specific surface area of the atovaquone particles and/or its solubility in adequate solvents or micelles to facilitate its dispersion in aqueous media.

Thus, one of the first works to increase the bioavailability of ATO was focused on reducing the particle size of the suspension. In this context, Dearn and co-workers demonstrated in male volunteers that the administration of microfluidized suspensions of 1  $\mu\text{m}$  average allowed to increase about 2.6-fold the oral relative bioavailability than when a conventional suspensions (of about 3  $\mu\text{m}$ ) was used (Dearn 2000). In another interesting study, Sek and collaborators examined the impact of a range of surfactants on the oral bioavailability of lipid based formulations of atovaquone (Sek et al. 2008). No differences were observed in beagle dogs when comparing two different self-microemulsifying drug delivery systems (SMEDDS) comprising long chain glycerides, ethanol and either Cremophor EL or Pluronic L121. On the contrary, the relative oral bioavailability in dogs of atovaquone was about 3-fold higher when incorporated in these SMEDDS than when formulated as aqueous suspension.

Another interesting possibility can be the association of this drug with bioadhesive nanoparticles. In this case the strategy would be to combine an increase of the specific surface area of the drug delivery system with the ability of these nanoparticles to develop adhesive interactions within the gut mucosa (Agüeros et al. 2009). In this context, our strategy has been the encapsulation of atovaquone in PVM/MA nanoparticles by the intervention of cyclodextrins.

Before the development of the nanoparticles containing atovaquone, the affinity of the drug with different cyclodextrins was evaluated. The phase-solubility analysis allowed us to determine not only the affinity between atovaquone and cyclodextrin, but also the stoichiometry between oligosaccharide and drug. In our case, the diagrams mainly showed phase solubility profiles type  $A_L$ . The values of  $K_{1:1}$  obtained for the solubility studies demonstrated that practically all the drug in solution would be forming complexes with the different cyclodextrins. The CE values confirm the higher affinity of atovaquone for methylated cyclodextrins than for other derived beta cyclodextrins (rank order was as follows: DMCD>RMCD>HPCD>SBECD). This fact can be explained by the higher lipophilicity of methylated cyclodextrins than hydroxypropylated ones (Brewster and Loftsson 2007).

For the preparation of nanoparticles, in a preliminary study, two different procedures were tested. First, atovaquone-cyclodextrin complexes were incubated with the polymer prior the formation of nanoparticles by desolvation. Second, nanoparticles were formed after the incubation of free atovaquone and cyclodextrin with the polymer (see Methods). Both procedures yielded nanoparticles with similar physico-chemical properties (data not shown) and the

second method was selected for the preparation of atovaquone-loaded nanoparticles. These carriers displayed a size ranging from 200 to 260 nm. These results are similar to those described for polymer nanocapsules by Cauchetier and collaborators (Cauchetier et al. 2003). In this work, they studied the influence of different poly(ester) on the physico-chemical properties of nanocapsules containing atovaquone dissolved in benzylbenzoate. In this case, nanocapsules were produced by interfacial deposition and the encapsulation efficiency was slightly higher than those reported here for PVM/MA nanoparticles (about 97% vs 80-87%). In any case, these encapsulation efficiencies in nanoparticles were higher than those reported for liposomes (Cauchetier et al. 2000).

For in vivo studies, only nanoparticles prepared with DMCD and HPCD were used. This selection was based on the physico-chemical properties of nanoparticles. Both ATO-HPCD-NP and ATO-DMCD-NP formulations displayed high yield and ATO loading values. These formulations were orally administered to animals as a single dose of 2.5 mg/kg. As a control, pulverised atovaquone was homogeneously dispersed in an aqueous solution of methylcellulose. The resulting suspension showed a mean particle diameter of about 640 nm, which was smaller than particle sizes previously reported by other research groups (Rolan et al. 1994; Dearn 2000; Dixon et al. 1996).

The pharmacokinetic study was carried out in rats to study the effect of nanoparticles formulations on the oral bioavailability of atovaquone. Blood samples were taken during the first 24 hours after the administration. Under these experimental conditions, the intravenous pharmacokinetic was

characterized by a slow removal of the drug with a long half-life. In previous works, it has been suggested that atovaquone is mainly eliminated unchanged in bile, suffering from enterohepatic recirculation (Baggish and Hill 2002). This fact can explain the presence of a secondary peak in the plasmatic curve of atovaquone, 6 hours after administration by the intravenous route (Figure 3).

On the other hand, all the oral treatments were characterised by an increase of the plasmatic drug concentration till the  $C_{max}$  was obtained, followed by a slow decline of atovaquone plasma concentrations. Concerning the  $T_{max}$ , little differences were found; although the highest  $T_{max}$  was observed for animals treated with ATO-DMCD NP. Similarly,  $C_{max}$  for this formulation was found to be significantly higher than for the control suspension ( $p < 0.05$ ). Overall, nanoparticle formulations induced higher and more prolonged plasmatic levels of atovaquone than control suspensions. This fact can be explained for ability of poly(anhydride) nanoparticles to strongly interact with the gut mucosa, which provokes an increase of the residence time and a slower release of the drug in the absorption site. On the contrary, the incorporation of empty nanoparticles in the atovaquone suspension did not increase the drug bioavailability, which confirms the need of an efficient drug encapsulation into the nanoparticles to promote the absorption of the antiprotozoan. The calculated relative oral bioavailability of atovaquone was found to be between 1.6 and 2.2-times higher for nanoparticle formulations than for the control suspension.

Comparing both types of nanoparticle formulations, carriers prepared in the presence of DMCD (ATO-DMCD NP) induced a higher drug bioavailability (70% vs 50%) than those prepared with HPCD (ATO-HPCD NP). This fact could be

explained by the higher complex affinity of atovaquone with DMCD than with HPCD (see Table 1). Thus, once the ATO-cyclodextrin complex was released in the mucosa medium, atovaquone would be dissociated more rapidly from HPCD than from DMCD complexes. Under these circumstances, it can be hypothesized that a dissociation rate of complexes higher than the absorption rate of atovaquone would favour the precipitation of a portion of the released drug. A schematic representation of this mechanism is shown in Figure 5.

## **Conclusions**

The use of cyclodextrins as “promoter” of encapsulation seems to be an appropriate strategy to increase the atovaquone loading in poly(anhydride) nanoparticles. In addition, the combination between PVM/MA (the copolymer between methyl vinyl ether and maleic anhydride) and DMCD (2,6-di-O-methyl- $\beta$ -cyclodextrin) enabled us to obtain poly(anhydride) nanoparticles capable of offering an atovaquone relative bioavailability close to 72%, which was found to be about 2.2 times higher than for the control suspension.

## **Acknowledgements**

This work was supported by the Foundation “Caja Navarra: Tú eliges, tú decides” (Nanotechnology and Medicines, number 10828) in Spain. Javier Calvo was also financially supported by GlaxoSmithKline I+D and “Fundación Universidad Empresa” (CITIUS grant) in Spain.

## References

M. Agüeros, P. Areses, M.A. Campanero, H. Salman, G. Quincoces, I. Penuelas, J.M. Irache, *Eur. J. Pharm. Sci.* 37, 231 (2009a)

M. Agüeros M, L. Ruiz-Gatón L, C. Vauthier C, K. Bouchemal K, S. Espuelas S, G. Ponchel G, J.M. Irache, *Eur. J. Pharm. Sci.* 38, 405 (2009b)

F.J. Araujo, J. Huskinson, J.S. Remington, *Antimicrob. Agents Chemother.* 35, 293 (1991)

P. Arbós, M. Wirth, M.A. Arangoa, F. Gabor, J.M. Irache, *J. Control. Release* 83, 321 (2002)

A.L. Baggish, D.R. Hill, *Antimicrob. Agents Chemother.* 46, 1163 (2002)

M.E. Brewster, T. Loftsson, *Adv. Drug Del. Rev.* 59, 645 (2007)

E. Cauchetier, M. Paul, D. Rivollet, H. Fessi, A. Astier, M. Deniau, *Int. J. Parasitol.* 30, 777 (2000)

E. Cauchetier, P.M. Loiseau, J. Lehman, D. Rivollet, J. Fleury, A. Astier, *Int. J. Parasitol.* 32, 1043 (2002)

E. Cauchetier, M. Paul, D. Rivollet, H. Fessi, A. Astier, M. Deniau, *Annals. Trop. Med. Parasitol.* 97, 259 (2003)

D. Cotton, *AIDS Clin. Care* 7, 62 (1995).

F. Dalençon, Y. Amjaud, C. Lafforgue, F. Derouin, H. Fessi, *Int. J. Pharm.* 153, 127 (1997)

A.R. Dearn, US Patent number 6649659 (2000)

R. Dixon, A.L. Pozniak, H.M. Watt, P. Rolan, J. Posner, *Antimicrob. Agents Chemother.* 40, 556 (1996)

J.B. Dressman, C. Reppas, *Eur. J. Pharm. Sci.* 11, S73 (2000)

D.J. Ferguson, J. Huskinson-Mark, F.G. Araujo, J.S. Remington, *Int. J. Exp. Pathol.*, 75, 111 (1994)

GlaxoSmithKline. Wellvone 750mg/5mL oral suspension [Online]. Available at: <http://www.medicines.org.uk/EMC/medicine/777/SPC/Wellvone%20750mg%205ml%20oral%20suspension/#FORM>. Accessed on 10 January 2011.

W.E. Gutteridge, *J. Protozool.* 38,141 (1991)

T. Higuchi, K.A. Connors, *Adv. Anal. Chem. Instrum.* 4, 117 (1965)

A.T. Hudson, *Parasitol. Today* 9, 66 (1993)

W.T. Hughes, W. Kennedy, J.L. Shenep, P.M. Flynn, S.V. Hetherington, G. Fullen, D.J. Lancaster, D.S. Stein, S. Palte, D. Rosenbaum, *J. Infect. Dis.* 163, 843 (1991)

W.T. Hughes, G. Leoung, F. Kramer, S. Bozzette, S. Safrin, P. Frame, N. Clumack, H. Masur, D. Lancaster, C. Chan, *N. Engl. J. Med.* 328, 1521 (1993)

I. Ittarat, W. Asawamahasakda, M.S. Bartlett, J.W. Smith, S.R. Meshnick, *Antimicrob. Agents Chemother.* 39, 325 (1995)

J.J. Kessl, B.B. Lange, T. Merbitz-Zahradnik, K. Zwicker, P. Hill, B. Meunier, H. Pálsdóttir, C. Hunte, S. Meshnick, B.L. Trumppower, *J. Biol. Chem.* 278, 31312 (2003)

J.J. Kessl, S.R. Meshnick, B.L. Trumppower, *Trends Parasitol.* 23, 494 (2007)

J.A. Kovacks, *Lancet* 340, 637 (1992)

T. Loftsson T, D. Hreindsdóttir D, M. Másson, *Int. J. Pharm.* 302, 18 (2005)

S. Looareesuwan, C. Viravan, H.K. Webster, D.E. Kyle, D.B. Hutchinson, *Am. J. Trop. Med. Hyg.* 54, 62 (1996).

A. Matsuu, Y. Koshida, M. Kawahara, K. Inoue, H. Ikadai, Y. Hikasa, S. Okano, S. Higuchi, *Vet. Parasitol.* 124, 9 (2004)

H.W. Murray, J. Hariprashad, *Antimicrob. Agents Chemother.* 40, 586 (1996)

E. Nicolaidis, E. Galia, C. Efthymiopoulos, J.B. Dressman, C. Reppas, *Pharm. Res.* 16, 1876 (1999)

S.N. Patel SN, K.C. Kain, *Expert Rev. Anti. Infect. Ther.* 3, 849 (2005)

M.E. Polhemus, S. Remich, B. Ogutu, J. Waitumbi, M. Lievens, W.R. Ballou, D.G.Jr. Heppner, *Antimicrob. Agents Chemother.* 52, 1493 (2008).

G. Ponchel, J.M. Irache, *Adv. Drug Del. Rev.* 34, 191 (1998).

P.D. Radloff, J. Phillips, M. Nkeyi, *Lancet* 347, 1511 (1996)

P.E. Rolan, A.J. Mercer, B.C. Weatherley, T. Holdich, R.W. Peck, G. Ridout, J. Posner, *Br. J. Clin. Pharmacol.* 37, 13 (1994)

S. Romand, M. Pudney, F. Derouin, *Antimicrob. Agents Chemother.* 37, 2371  
(1993)

L. Sek, B.J. Boyd, W.N. Charman, C.J. Porter, *J. Pharm. Pharmacol.* 58,809  
(2008)

I.W. Sherman, *Adv. Parasitol.* 67, 101 (2009)

C.M. Spencer, K.L. Goa, *Drugs* 50, 176 (1995)

F. Sordet, Y. Aumjaud, H. Fessi, F. Derouin, *Parasite* 3,223 (1998)

## Figure captions

Figure 1. Phase-solubility diagrams of atovaquone-cyclodextrin systems in PBS at 25°C. Data shown the amount of atovaquone ([ATO]) solubilised as a function of the amount of cyclodextrin ([CD]) added (○ DMCD / □ RMCD / ■ HPCD / ▲ SBECD). The experiment was performed in triplicate (n = 3). DMCD: 2,6-di-O-methyl-β-cyclodextrin; RMCD: randomly methylated β-cyclodextrin; HPBCD: 2-hydroxypropyl-β-cyclodextrin; SBECD: sulfobutyl ether-β-cyclodextrin.

Figure 2. Microphotographs of ATO-RMCD NP (A), ATO-HPCD NP (B) and ATO-DMCD NP (C) obtained by scanning electron microscopy (SEM). Magnification: x 25,000. ATO-RMCD NP: ATO-loaded RMCD/poly(anhydride) nanoparticles; ATO-HPCD NP: ATO-loaded HPMC/poly(anhydride) nanoparticles; ATO-DMCD NP: ATO-loaded DMCD/poly(anhydride) nanoparticles.

Figure 3. Pharmacokinetics of atovaquone after an intravenous administration to rats. Animals received an intravenous dose of 150 µg/kg formulated in DMSO/HPCD/saline. Error bars represent standard deviation from the mean (n=5).

Figure 4. Atovaquone plasmatic levels after the oral administration of a single dose of 2.5 mg/kg. Animals received the drug formulated in either nanoparticles (ATO-DMCD NP; ◆, ATO-HPCD NP; ◇), 1% methylcellulose suspension (ATO-

MC; ●) or 1% methylcellulose suspension containing empty nanoparticles (ATO-MC+NP; Δ). Error bars represent standard deviation from the mean (n=5).

Figure 5. Representation of the hypothetical mechanism by which the presence of DMCD in poly(anhydride) nanoparticles would improve the absorption of atovaquone.  $K_d$ : dissociation constant;  $K_a$ : absorption rate; DMCD:ATO: inclusion complex between 2,6-di-O-methyl- $\beta$ -cyclodextrin and atovaquone. HPCD:ATO: inclusion complex between 2-hydroxypropyl- $\beta$ -cyclodextrin and atovaquone.

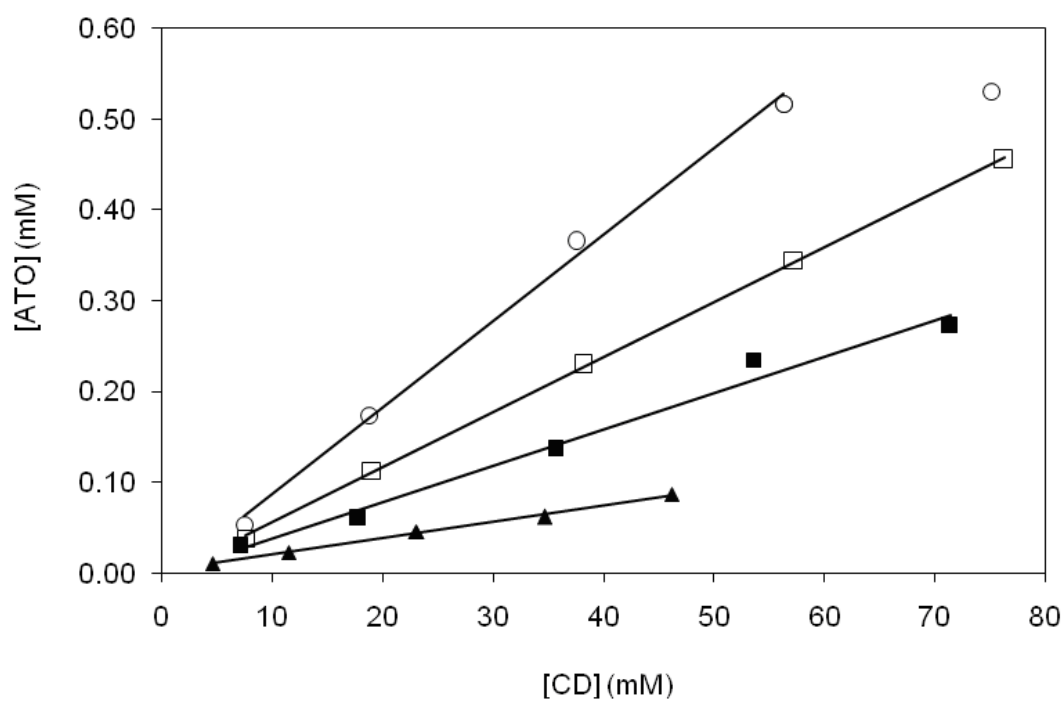


Figure 1.

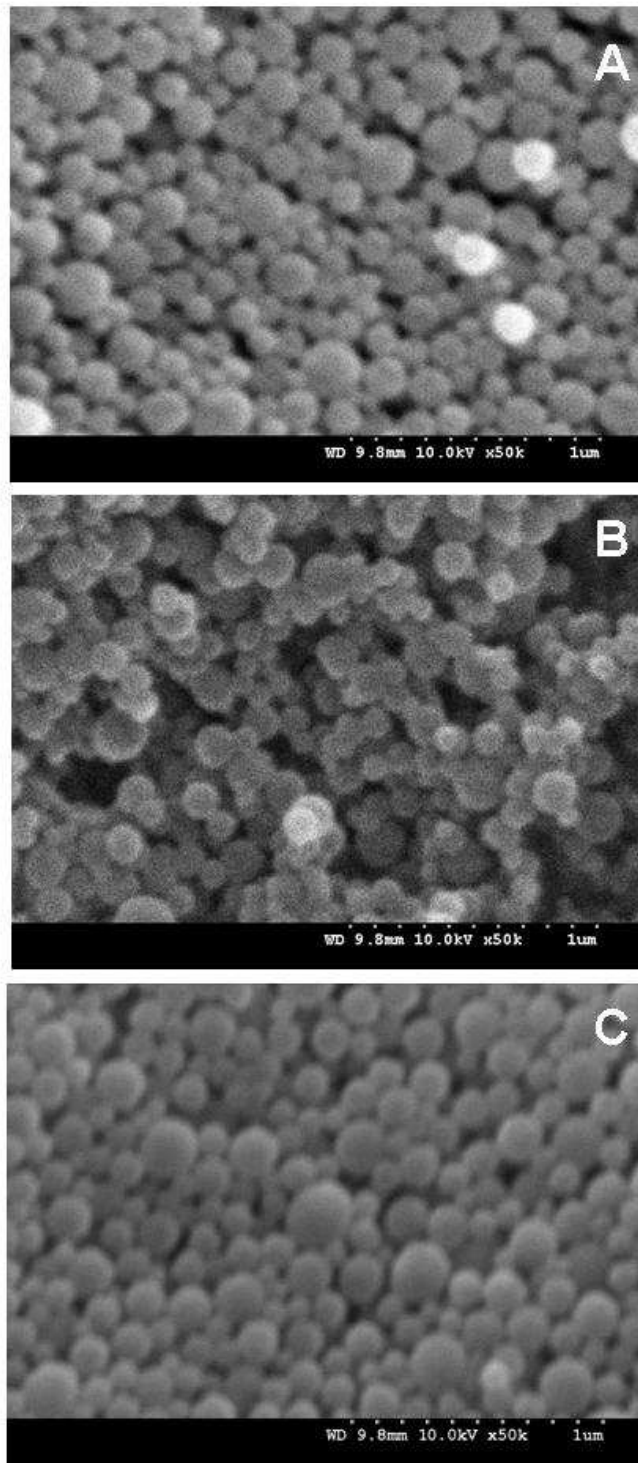
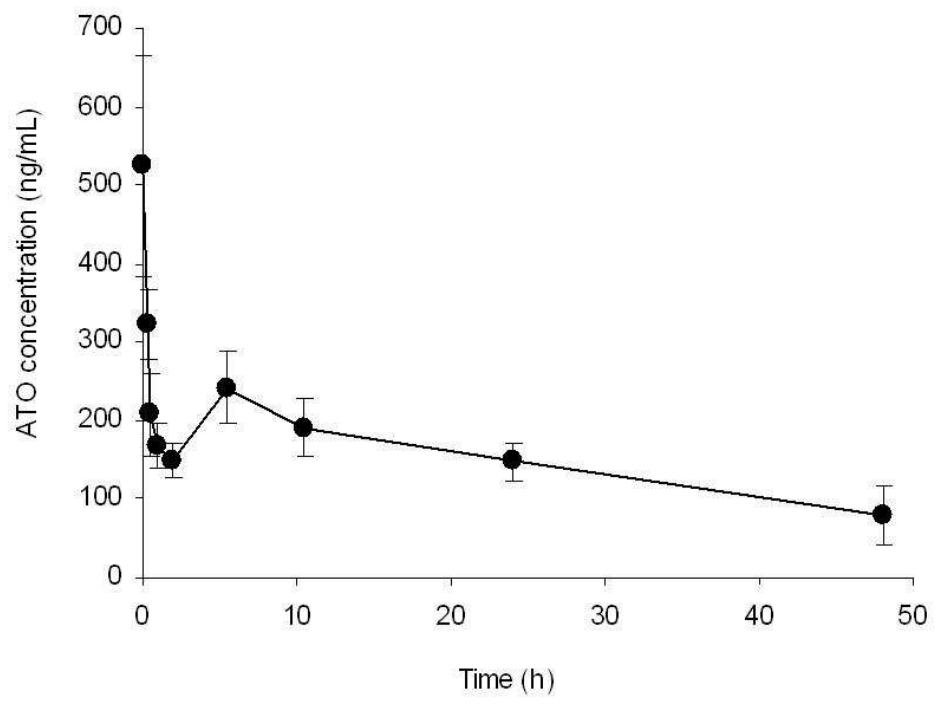


Figure 2



**Figure 3.**

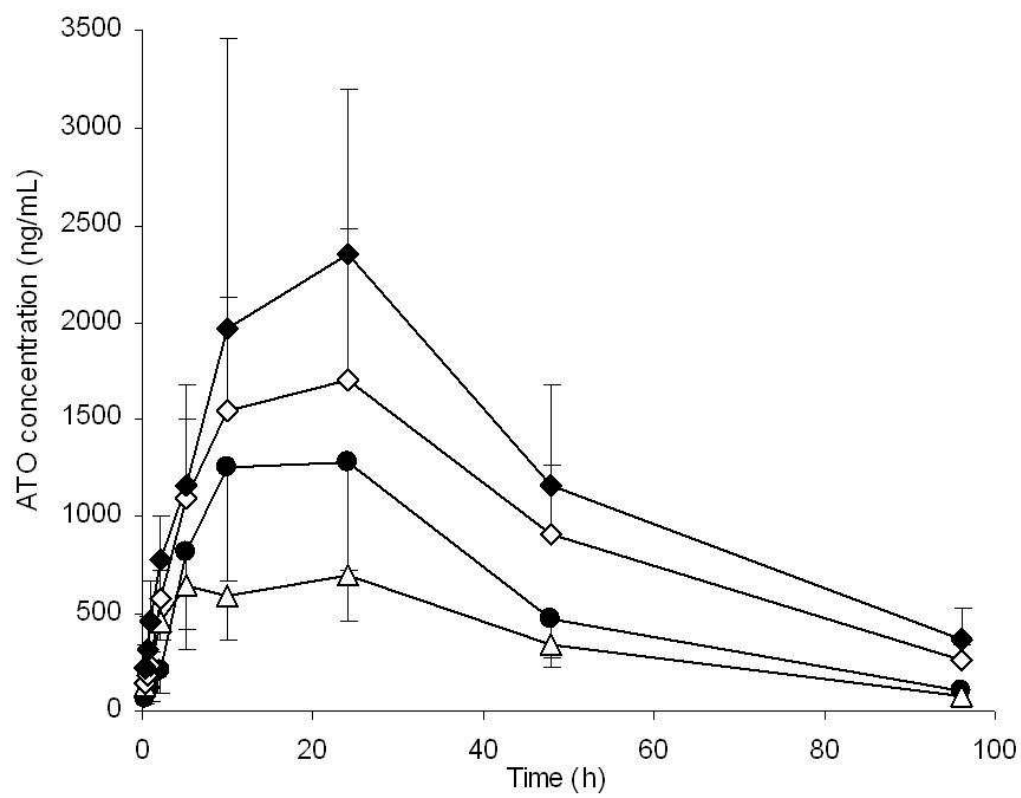


Figure 4.

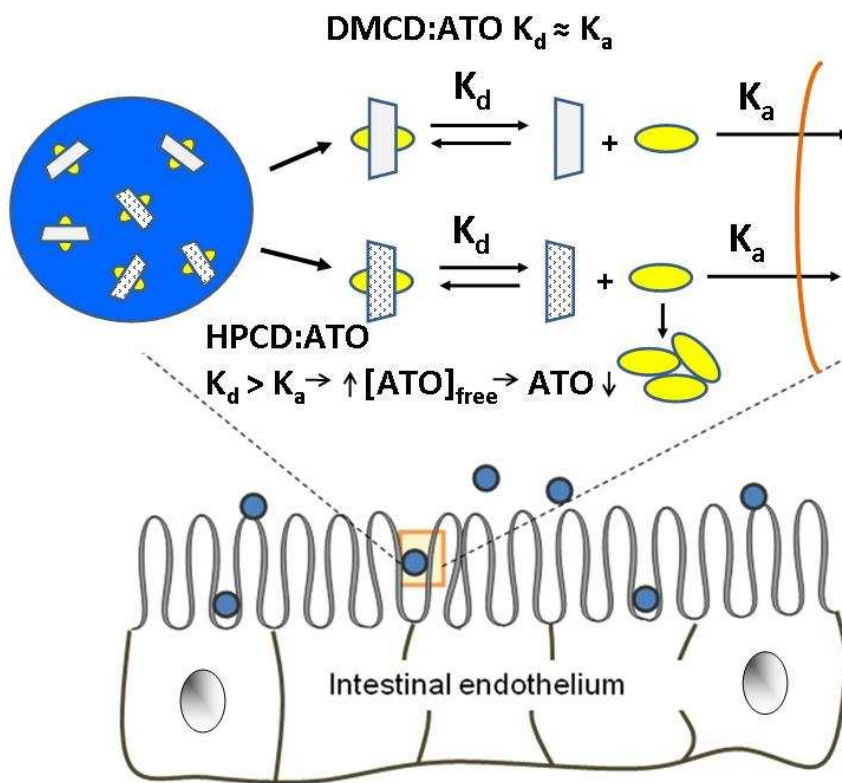


Figure 5.

**Table 1.** Phase-solubility study: slope of curves, solubility of atovaquone in aqueous phosphate buffer containing 10% w/v cyclodextrin ( $S_{CD}$ ), apparent stability constant ( $K_c$ ) and complexation efficiency (C.E.).

<b>Cyclodextrin</b>	<b>Slope</b>	<b><math>S_{CD}</math> (<math>\mu\text{M}</math>)</b>	<b><math>K_c</math> (<math>\text{M}^{-1}</math>)</b>	<b>C.E.</b>
HPCD	0.004	262.8	3300	0.004
RMCD	0.006	444.6	5300	0.006
DMCD	0.010*	520.4	6400	0.010
SBECD	0.002	76.7	950	0.002

(\*) Slope calculated using the linear portion of the curve.

**Table 2.** Physico-chemical characteristics of the different poly(anhydride) nanoparticles. Data expressed as the mean  $\pm$  SD (n=3). ATO-MC: atovaquone dispersed in 1% methylcellulose suspension; NP: empty poly(anhydride) nanoparticles; ATO-HPCD NP: ATO-loaded HPMC/poly(anhydride) nanoparticles; ATO-RMCD NP: ATO-loaded RMCD/poly(anhydride) nanoparticles; ATO-DMCD NP: ATO-loaded DMCD/poly(anhydride) nanoparticles.

	<b>Size<sup>a</sup></b> (nm)	<b>PDI</b>	<b>Zeta potential<sup>b</sup></b> (mV)	<b>Yield<sup>c</sup></b> (%)	<b>ATO loading</b> ( $\mu$ g ATO/mg NP)	<b>EE<sup>d</sup></b> (%)
ATO-MC	641 $\pm$ 6	0.127	-	-	-	-
NP	240 $\pm$ 5	0.165	-51.1 $\pm$ 3.2	82.05	< 0.1	< 0.1
ATO-HPCD NP	199 $\pm$ 3	0.056	-48.1 $\pm$ 1.7	77.39	16.9 $\pm$ 1.2	82.77
ATO-RMCD NP	259 $\pm$ 2	0.177	-44.3 $\pm$ 2.6	69.12	12.74 $\pm$ 2.5	77.72
ATO-DMCD NP	256 $\pm$ 3	0.195	-46.6 $\pm$ 5.2	78.73	17.82 $\pm$ 0.9	87.33

<sup>a</sup> Determination of the nanoparticle size (nm) by photon correlation spectroscopy.

<sup>b</sup> Determination of the zeta potential (mV) by electrophoretic laser Doppler anemometry.

<sup>c</sup> Percentage of polymer transformed into nanoparticles.

<sup>d</sup> EE: Encapsulation efficiency

**Table 3.** Pharmacokinetic parameters of atovaquone in rats for the different formulations tested. ATO-MC: atovaquone dispersed in 1% methylcellulose suspension; ATO-MC + NP: physical mixture between empty poly(anhydride) nanoparticles and 1% methylcellulose suspension; ATO-DMCD NP: ATO-loaded DMCD/poly(anhydride) nanoparticles; ATO-HPCD NP: ATO-loaded HPMC/poly(anhydride) nanoparticles. Animals received a single oral dose of 2.5 mg/kg.

<b>Formulation</b>	<b>C<sub>max</sub><sup>a</sup></b> ( $\mu\text{g ml}^{-1}$ )	<b>T<sub>max</sub><sup>b</sup></b> (h)	<b>AUC<sub>0-∞</sub><sup>c</sup></b> ( $\mu\text{g ml}^{-1}\text{min}^{-1}$ )	<b>MRT<sup>d</sup></b> (h)	<b>F<sub>rel</sub><sup>e</sup></b> (%)
ATO-MC	1.36 ± 0.59	14.6	58.87 ± 29.10	31.38 ± 2.06	31.81
ATO-MC + NP	0.72 ± 0.26	17.4	38.22 ± 9.84	33.65 ± 2.13	20.65
ATO-HPCD NP	1.90 ± 0.72	15.6	96.79 ± 29.25	36.31 ± 1.90	52.30
ATO-DMCD NP	2.71 ± 1.22*	18.4	131.91 ± 56.61*	37.09 ± 1.15	71.28

<sup>a</sup> Peak plasma concentration

<sup>b</sup> Time to reach C<sub>max</sub>

<sup>c</sup> Area under the plasma concentration-time curve

<sup>d</sup> Mean residence time

<sup>e</sup> Relative oral bioavailability.

\* p<0.05 ATO-DMCD NP vs ATO-MC. Test U – Mann Whitney.